Available online at www.sciencedirect.com
ScienceDirect
Journal of Power Sources 182 (2008) 422–428
JOURNAL OF POWER SOURCES
www.elsevier.com/locate/jpowsour

The impact of air contaminants on PEMFC performance and durability

Yoshiki Nagahara *, Seiho Sugawara, Kazuhiko Shinohara

Fuel Cell Laboratory, Nissan Research Center, Nissan Motor Co. Ltd., 1 Natsushima-cho, Yokosuka-shi, Kanagawa 237-8523, Japan

Received 31 October 2007; received in revised form 14 December 2007; accepted 14 December 2007
Available online 4 January 2008

Abstract

The impact of air contaminants such as sulfur compounds (SO_2, H_2S) and nitrogen compounds (NO_x and NH_3) was investigated using subscale fuel cells. The severity of the effect of these impurities varies depending on the contaminants. Among air contaminants, sulfur compounds cause the most severe performance loss due to decrease of available Pt sites for oxygen reduction reaction (ORR). We found that sulfur compounds adsorbed on Pt surface tend to be oxidized to sulfate at 0.9 V and higher potentials. The cell performance can be recovered partially by excursions to high potentials due to increase of available Pt sites. Furthermore, flushing the cathode with high humidity gases results in almost complete recovery of the cell performance. We conclude that these recovery effects are due to oxidation/removal of the contaminants from the Pt surface.

Keywords: PEMFC; Air contaminant; SO_2; Poisoning; Durability; Recovery

1. Introduction

PEMFCs today typically use highly dispersed Pt/C as the catalyst on both the anode and the cathode. Pt is a good catalyst for both HOR and ORR but is easily susceptible to poisoning by various contaminants found in both the fuel and air. Contaminants present in the atmosphere include sulfur compounds (SO_2, H_2S) and nitrogen compounds (NO_2, NO). The major sources of these contaminants are the automotive vehicle exhaust and industrial manufacturing processes. For example, the annual average concentrations of SO_2 and NO_2 in the atmosphere in Japan based on the roadside air pollution monitoring stations data are 4 ppb and 27 ppb, respectively [1]. However, in the case of fuel cell vehicles (FCV), we should take into account the concentrations of contaminants at various places. For example, near hot springs, the SO_2 and H_2S concentration can occasionally reach several hundred ppb. So far, various studies concerning the effect of air contaminants on the performance of PEMFCs have been reported in the literature. It has been demonstrated that intrusion of NO_2/air could cause the cell performance loss, but the cell performance could be almost completely recovered after stopping NO_2 injection [2–5]. On the other hand, the cell performance decayed after running in the presence of SO_2/air and could not be recovered by stopping SO_2 intrusion [2,3]. Recently, Jing et al. [6] researched the cathode contamination and also indicated that even 1 ppm SO_2 in air can seriously affect the performance of PEMFCs and the SO_2 poisoned cell performance can be recovered only partially by neat air supply. The recovery of the cell performance that has been degraded due to SO_2 poisoning has been shown to be possible by excursions to extremely high potentials (>1.4 V) [2,4]. However, excursions to such high potentials can also accelerate the degradation and corrosion of other materials such as carbon. Therefore an alternative method for recovery is needed in order to improve the SO_2 poisoning durability of PEMFCs. In this paper, our results on the investigation of the impact of air contaminants, especially SO_2 using subscale fuel cells are presented.

2. Experimental

All experiments were conducted using subscale single cell (active area of 25 cm^2). The MEA used was PRIMEA® Series 5570 (JAPAN GORE-TEX Inc.) which has 0.4 mg cm^{-2} Pt on both the anode and the cathode. Gas diffusion layers (GDLs)

* Corresponding author. Tel.: +81 46 867 5331; fax: +81 46 867 5332.
E-mail address: y-nagahara@mail.nissan.co.jp (Y. Nagahara).

0378-7753/$ – see front matter © 2007 Elsevier B.V. All rights reserved.
doi:10.1016/j.jpowsour.2007.12.091

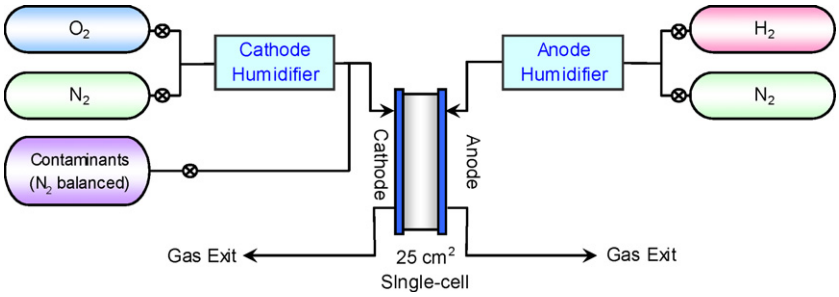

Fig. 1. Schematic representation of single cell test station.

were CARBEL CFP200 (thickness of 200 μm, JAPAN GORE-TEX Inc.). Test stations made by Chino Corporation (Tokyo, Japan) were used for all experiments. Fig. 1 shows the schematics for testing. The gases used were high purity H_2 (99.995%) for the anode feed, high purity O_2 (99.9999%) for the cathode feed and high purity N_2 (99.9999%) for both the anode and the cathode feed. For the H_2/air measurements, simulated air produced by mixing 79.1% high purity N_2 and 20.9% high purity O_2 was supplied to the cathode. These gases were humidified in a bubbling humidifier before entering the fuel cell. In the poisoning durability test, the designated concentrations of gaseous contaminants (SO_2, H_2S, NO, NO_2 and NH_3) were premixed with humidified simulated air or high purity N_2 and then supplied to the cathode. The durability test conditions are presented in Table 1. The decay in the voltage during continual injection of air/contaminants to the cathode at a constant current (1 A cm^{-2}) was measured. For comparison of the impact of various contaminants, durability tests at constant current with injection of 0.5 ppm SO_2, 0.6 ppm H_2S, 2 ppm NO, 2 ppm NO_2 and 5 ppm NH_3 were conducted. These high concentrations were set to accelerate the effects of each contaminant. Furthermore, we focused our work on the SO_2 poisoning phenomena in detail and conducted the durability tests with low concentration (50 ppb) SO_2 injection. In order to evaluate the negative effect of contaminants on ORR catalytic activity and behavior of contaminants on Pt surface, we performed *I–V* measurements and cyclic voltammetry before and after the durability test. For cyclic voltammetry, humidified high purity H_2 was used on the anode (counter and reference electrode), and humidified high purity N_2 was used on the cathode (working electrode). The cell temperature was 80 °C and the humidification temperatures were 80 °C/80 °C (100/100%RH). The gas flow rate was 0.5/0.5 dm^3 min^{-1}. The applied potential range was between 0.04 and 0.9 V. The scan rate used was 50 mV s^{-1}. Following the cyclic voltammetry, *I–V* curves were measured in both H_2/air and H_2/O_2 conditions. The cell temperature was 80 °C and the humidification temperatures were 63.8 °C/63.8 °C (50/50%RH). The current range for *I–V* measurements was between 0 and 27.5 A (1.1 A cm^{-2}), gas flow rate corresponding to a stoichiometry of 1.5/1.5 for H_2/air and 1.5/7.5 for H_2/O_2 at each current was controlled. In addition, we attempted high humidity operation using H_2/O_2 at 100% RH for the recovery of the cell performance following the durability test. The operating conditions are presented in Table 2.

In addition to the constant current durability test, we also performed the constant potential durability test in order to investigate the SO_2 poisoning dependence on potential. The test conditions are shown in Table 3. Humidified high purity H_2 was used for the anode feed, and 2 ppm SO_2/N_2 was used for the cathode feed. The cell temperature was 80 °C and the humidification temperatures were 80 °C/80 °C (100/100%RH). The gas flow rate was 0.5/0.5 dm^3 min^{-1}. The cathode potential was held at constant potential (0.5–0.9 V) and cyclic voltammetry was performed every 20 min until total holding time reached 120 min. The upper limit potential of the cyclic voltammetry

Table 1
Constant current durability test condition

Cell temperature (°C)	80
Pressure	Ambient
Gas (A/C)	H_2/air + contaminant
Gas RH (A/C) (%)	50/50
Gas FR (A/C) (dm^3 min^{-1})	0.261/0.625
Current density (A cm^{-2})	1
Duration (h)	45

Table 2
High humidity operation condition

Cell temperature (°C)	80
Pressure	Ambient
Gas (A/C)	H_2/O_2
Gas RH (A/C) (%)	100/100
Gas FR (A/C) (dm^3 min^{-1})	0.5/1.2
Current density (A cm^{-2})	1
Duration (h)	2

Table 3
Constant potential durability test condition

Cell temperature (°C)	80
Pressure	Ambient
Gas (A/C)	H_2/N_2 + 2 ppm SO_2
Gas RH (A/C) (%)	100/100
Gas FR (A/C) (dm^3 min^{-1})	0.5/0.5
Holding potential (V)	0.5, 0.6, 0.7, 0.8, 0.9
Sweep rate (mV s^{-1})	50
1st vertex potential (V)	0.04
2nd vertex potential	Same as holding potential
Total holding time (min)	180

was set to the same as holding potential in order to avoid the influence of higher potentials than holding potential.

3. Results and discussions

3.1. Constant current durability test

3.1.1. Comparison of various air contaminants

Fig. 2 shows the change of cell voltage at 1 A cm^{-2} during continuous injection of various air contaminants (0.5 ppm SO_2, 0.6 ppm H_2S, 2 ppm NO, 2 ppm NO_2 and 5 ppm NH_3) mixed with humidified simulated air to the cathode. The horizontal axis in Fig. 2 represents the cumulative injection of contaminants. On comparing curves in Fig. 2, voltage decay caused by sulfur compounds was found to be much more severe than that by nitrogen compounds even though the concentration of sulfur compounds injected was lower than that of nitrogen compounds. The oxidation state of sulfur compounds (SO_2 or H_2S) did not appear to affect the performance decay rate. These trends are consistent with the results reported by Jing et al. [6]. The difference in the voltage decay between sulfur compounds and nitrogen compounds can be attributed to the difference in adsorption strength of contaminants on Pt surface. Several literatures [2,3,5] reported that the cell performance degraded due to sulfur compounds and was recovered only partially by operating with neat air. On the other hand, the cell performance degradation due to nitrogen compounds injection can be almost completely recovered by the same operation. We also performed the similar operation and obtained the similar results to theirs. These facts indicate that sulfur compounds are much more detrimental to PEMFC performance than nitrogen compounds. Therefore, in this paper, we have focused our work mainly on the SO_2 poisoning phenomena in detail.

3.1.2. Impact of low concentration SO_2 and effect of recovery operation

Fig. 3 shows the change of cell voltage measured during durability test and at *I–V* measurements. The cell voltage gradually decayed with time and decreased by 96 mV after 45 h of SO_2 injection. The cell voltage was partially recovered (i.e. increased by 57 mV) by *I–V* measurement using air for the cathode feed. After the high humidity operation for 2 h following the *I–V* measurement, further recovery effect was observed and the cell voltage was restored almost completely (i.e. increased by 37 mV more).

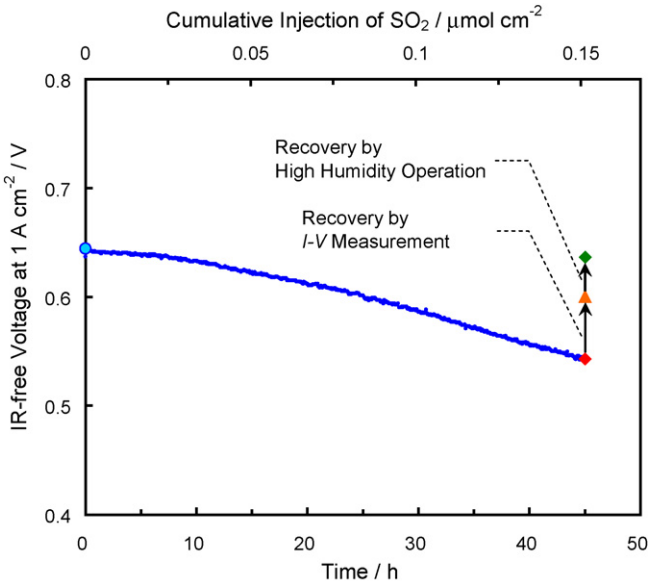

Fig. 3. Trend of the cell voltage at 1 A cm^{-2} during 50 ppb SO_2 injection to the cathode.

Fig. 4 shows comparison of *I–V* curves obtained using air for the cathode feed. The *I–V* curve measured after the durability test showed voltage decay at whole current density range but there was no steep voltage drop at high current density. Fig. 5

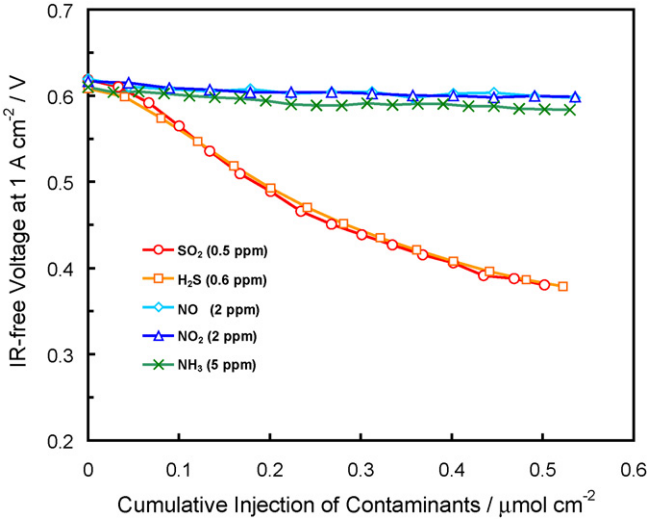

Fig. 2. Effect of various air contaminants on the cell voltage at 1 A cm^{-2}.

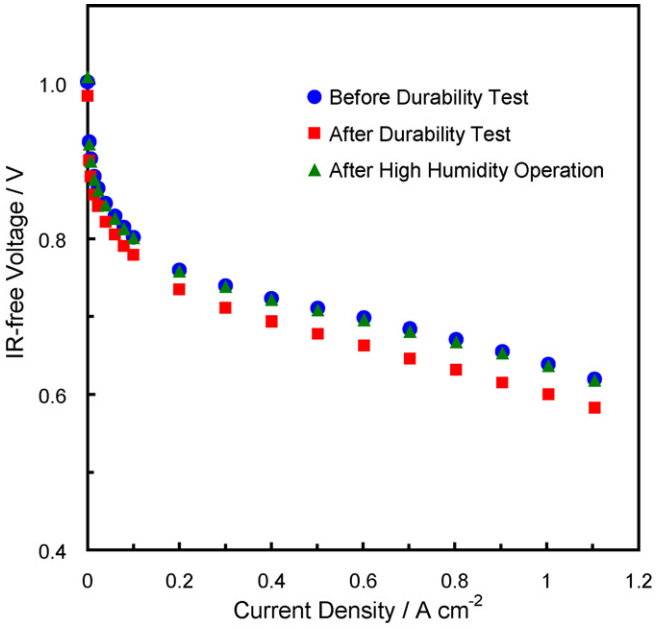

Fig. 4. Change of *I–V* curves measured using H_2/air.

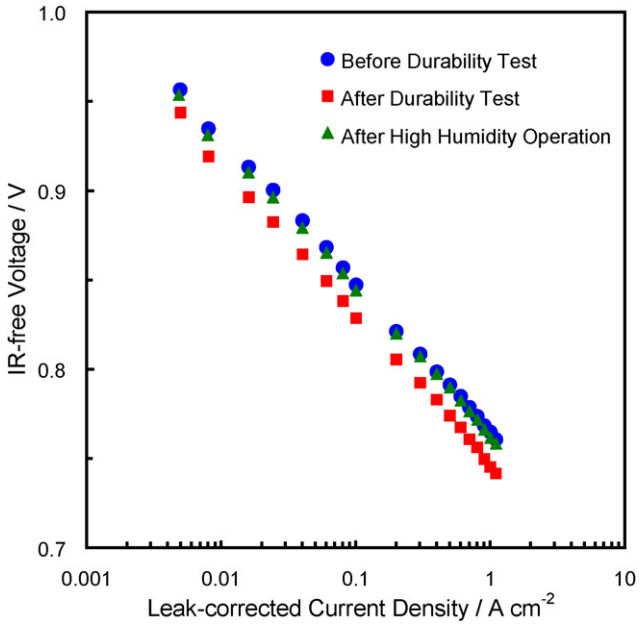

Fig. 5. Change of Tafel plots measured using H_2/O_2.

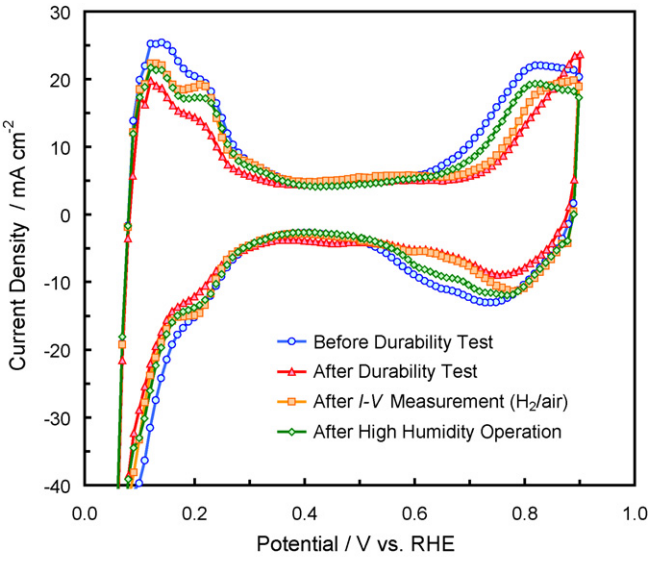

Fig. 6. Change of cyclic voltammograms of the cathode. Scan rate: 50 mV s^{-1}.

shows Tafel plots measured using O_2 for the cathode feed. These measurements were performed following the *I–V* measurement. Tafel plot after the durability test also indicated voltage decay at whole current density range. The voltage decay caused by SO_2

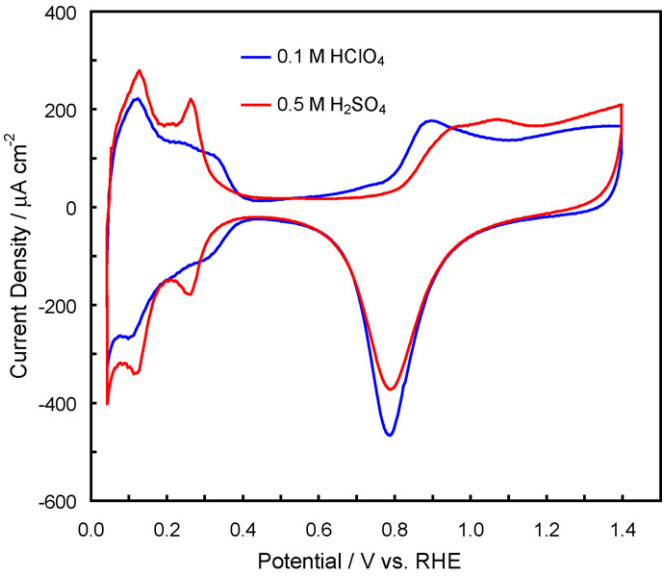

Fig. 7. Cyclic voltammograms of Pt measured in perchloric acid and sulfuric acid solutions. Scan rate: 50 mV s^{-1}.

injection can be considered to be due to increase of kinetic loss. The kinetic loss is probably attributed to available Pt surface area decreases due to sulfur species adsorption [2,6]. As shown in Figs. 4 and 5, after the high humidity operation, almost complete recovery of voltage in the entire current density range was observed in both measurements. The performance change can be attributed to the change of kinetic loss. In order to investigate the cause of kinetic loss, we compared the cyclic voltammograms measured in our work.

Fig. 6 shows the change of cyclic voltammograms. After the durability test, a decrease of the H-adsorption/desorption currents, a shift of the onset of Pt oxide formation to higher potentials, and a decrease of Pt oxide-reduction currents were observed. These changes suggest the existence of adspecies on the Pt surface. After the *I–V* measurement, the H-adsorption/desorption currents were greatly recovered, while the onset of Pt oxide formation hardly changed. A slight increase of Pt oxide-reduction currents was observed. Furthermore, new peaks appeared at around 0.2 V. After the high humidity operation, the onset of Pt oxide formation and Pt oxide-reduction currents were greatly recovered. The peaks at around 0.2 V disappeared. Table 4 shows the change of the cell performance and the charge density of H-desorption and Pt oxidation. The H-desorption charge density is generally used for estimation of Pt surface area. The Pt oxidation charge density was calculated by integration of oxidation current density from the

Table 4
The cell performance and the charge density of H-desorption and Pt oxidation

	IR-free voltage at 1 A cm^{-2} (endurance test) (V)	Current density at 0.9 V (H_2/O_2) (mA cm^{-2})	H-desorption charge density (mC cm^{-2})	Pt oxidation charge density at 0.9 V (mC cm^{-2})
Before endurance test	0.639	24.6	59.9	68.7
After endurance test	0.543	–	34.6	43.0
After *I–V* measurement	0.600	14.4	51.7	44.9
After humid operation	0.637	21.1	48.7	54.8

onset of Pt oxide formation to 0.9 V in cyclic voltammograms. The H-desorption charge density decreased due to SO_2 injection and was recovered by the *I–V* measurement. These trends are qualitatively consistent with the performance change. After the high humidity operation, further recovery of the cell performance was observed, while the H-desorption charge density hardly changed. The reason of performance recovery cannot be explained with H-desorption charge density change.

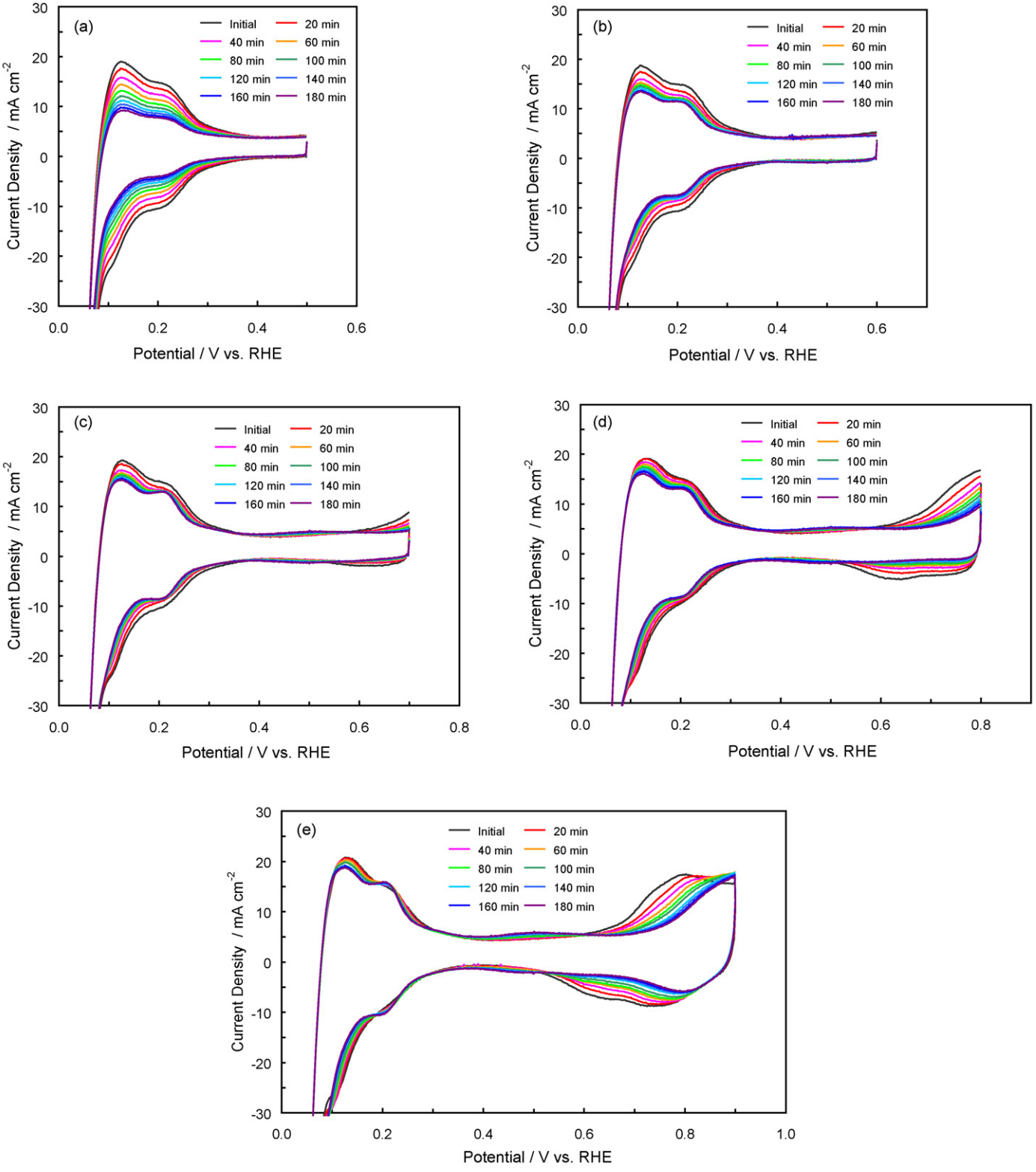

Fig. 8. Cyclic voltammograms measured in constant potential durability test: (a) 0.5 V hold; (b) 0.6 V hold; (c) 0.7 V hold; (d) 0.8 V hold; (e) 0.9 V hold.

Fig. 7 shows the cyclic voltammograms of polycrystalline platinum measured in 0.1 M $HClO_4$ and 0.5 M H_2SO_4 at a scan rate of 50 mV s^{-1}. All potentials were measured with respect to a reversible hydrogen electrode (RHE). In H_2SO_4, peaks at 0.25 V and a shift of the onset of Pt oxide formation can be seen. By comparing with cyclic voltammograms in Fig. 6, sulfate species can be considered to exist in the cathode catalyst layer after the *I–V* measurement since characteristics of the cyclic voltammograms are similar each other. Oxidation of sulfur adspecies to sulfate should occur during *I–V* measurement since the measurement procedure includes relatively high voltage (>0.9 V) period. It is reported that the sulfur adspecies are oxidized to sulfate (SO_4^{2-}) in aqueous phase during potential sweep up to 1.5 V [7–9]:

$$Pt\text{–}S + 4H_2O \leftrightarrow SO_4^{2-} + 8H^+ + 6e^- + Pt$$

After the high humidity operation, the peak current at 0.2 V decreased and the onset of Pt oxide formation got close to that measured before the durability test. Therefore, we think that the majority of sulfate in the cathode catalyst layer were removed by the high humidity operation. Schmidt et al. reported that sulfate specifically adsorbs on Pt surface and decreases the ORR activity [10].

Considering these facts, we suppose:

- SO_2 adsorbed strongly on Pt surface and caused an increase of kinetic loss.
- Oxidation of sulfur to sulfate by the *I–V* measurement decreased kinetic loss considerably, while the cell performance was not completely recovered due to specific adsorption of sulfate.
- Water condensation by high humidity operation washed out sulfate and restored the cell performance almost completely.

These changes are finally attributed to the number of available Pt sites for ORR during the operation. It is generally recognized that the H-adsorption/desorption charge is equivalent to Pt surface area. A decrease of number of available Pt sites due to specific adsorption of anion such as sulfate is not included in the H-adsorption/desorption charge since the peaks corresponding to these reactions can be observed at low potential. Since we did not measure the available Pt surface area directly, we regarded the Pt oxidation charge density as a representative of the number of available Pt sites during the operation as long as measuring same sample. As shown in Table 4, the change of cell performance change correlates with that of Pt oxidation charge density. Slight shortage to full recovery is observed especially in the charge density. It can be considered to be due to Pt particle growth which occurs at steady state operation [11,12].

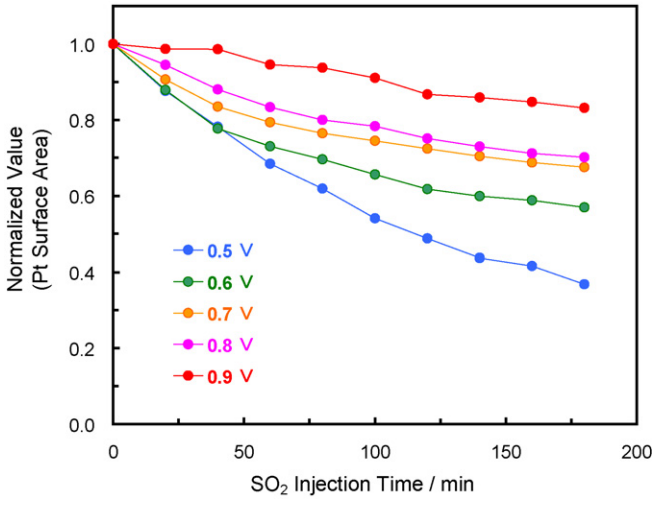

Fig. 9. Change of normalized Pt surface area as a function of potential holding time.

3.2. Constant potential durability test

Fig. 8 shows the change of cyclic voltammograms measured in constant potential durability test. In the case of 0.5 V hold (Fig. 8(a)), the H-adsorption/desorption currents significantly decreased with time. This change is due to decrease of Pt available sites by adsorption of sulfur species. It was seen that the H-adsorption/desorption currents decrease tends to be suppressed as the holding potential increased. At 0.9 V holding (Fig. 8(e)), the H-adsorption/desorption currents hardly changed, whereas the appearance of the peaks around 0.2 V and the shift of onset of Pt oxide formation were observed. These can be attributed to an increase of sulfate in cathode catalyst layer. Fig. 9 shows the change of Pt surface area derived by integration of H-desorption current density. This figure indicates that at the higher potential, the more the SO_2 adsorption is suppressed. Thus, we confirmed that sulfur adspecies tend to be oxidized to sulfate at 0.9 V or higher potential in single cells.

4. Conclusions

Among the various air contaminants investigated in this work, sulfur compounds cause the most severe performance loss by causing a decrease of available Pt sites for ORR reaction. Loss of performance can be attributed to kinetic losses. Sulfur compounds adsorbed on Pt tend to be oxidized to sulfate when held at 0.9 V or higher potential in fuel cell. The performance can be partially recovered by excursions to high potentials due to increased availability of Pt sites. The remaining performance loss can be attributed to the adsorption of sulfate generated by oxidation of sulfur adspecies. Furthermore, almost complete recovery of cell performance was achieved by flushing out of sulfate from the catalyst layer by the application of high RH.

Acknowledgements

The authors would like to acknowledge Dr. Shyam Kocha (Fuel Cell Laboratory, Nissan Research Center) for technical discussions and help with the manuscript. We also thank JAPAN GORE-TEX Inc. for providing us with the MEAs.

References

[1] FY 2005 Report on the State of Air Pollution, Ministry of the Environment, Government of Japan. http://www.env.go.jp/air/osen/jokyo_h17/index.html.
[2] R. Mohtadi, W.-K. Lee, J.W. Van Zee, J. Power Sources 138 (2004) 216–225.
[3] T.Q. Rockward, F. Uribe, Proceedings of the 208th Meeting of The Electrochemical Society, Los Angeles, CA, October, 2005 (Abstract 1175).
[4] F. Uribe, W. Smith, M. Wilson, FY 2003 Progress Report, LANL, January 2005.
[5] D. Yang, J. Ma, L. Xu, M. Wu, H. Wang, Electrochim. Acta 51 (2006) 4039–4044.
[6] F. Jing, M. Hou, W. Shi, J. Fu, H. Yu, P. Ming, B. Yi, J. Power Sources 166 (2007) 172–176.
[7] T. Loučka, J. Electroanal. Chem. 31 (1971) 319–332.
[8] C. Quijada, A. Rodes, J.L. Vázquez, J.M. Pérez, A. Aldaz, J. Electroanal. Chem. 394 (1995) 217–227.
[9] C. Quijada, A. Rodes, J.L. Vázquez, J.M. Pérez, A. Aldaz, J. Electroanal. Chem. 398 (1995) 105–115.
[10] T.J. Schmidt, U.A. Paulus, H.A. Gasteiger, R.J. Behm, J. Electroanal. Chem. 508 (2001) 41–47.
[11] M.S. Wilson, F.H. Garzon, K.E. Sickafus, S. Gottesfeld, J. Electrochem. Soc. 140 (1993) 2872–2877.
[12] D. Liu, S. Case, J. Power Sources 162 (2006) 521–531.